

Constraints for rare electron-capture decays mimicking detection of dark-matter particles in nuclear transitions

Aagrah Agnihotri* and Jouni Suhonen†

University of Jyväskylä, Department of Physics, P.O. Box 35, FI-40014 Jyväskylä, Finland

Hong Joo Kim‡

Department of Physics, Kyungpook National University, Daegu 41566, Republic of Korea

(Dated: December 25, 2024)

We give for the first time, theoretical estimates of unknown rare electron-capture (EC) decay branchings of ^{44}Ti , ^{57}Co , and ^{139}Ce , relevant for searches of (exotic) dark-matter particles. The nuclear-structure calculations have been done exploiting the nuclear shell model (NSM) with well-established Hamiltonians and an advanced theory of β decay. In the absence of experimental measurements of these rare branches, these estimates are of utmost importance for terrestrial searches of dark-matter particles, such as axionic dark matter in the form of axion-like particles (ALPs), anapole dark matter, and dark photons in nuclear transitions. Predictions are made for EC-decay rates of 2^{nd} -forbidden unique (FU) and 2^{nd} -forbidden non-unique (FNU) EC transitions that can potentially mimic dark-matter-particle detection in dedicated underground experiments designed to observe the absence of the corresponding nuclear electromagnetic transitions.

The study of nuclear β decays has important implications for Beyond the Standard Model Physics (BSMP) [1–5]. Among different avenues of searches for BSMP, where the study of nuclear β decays plays an important role, experimental searches for solar axions have long been among such endeavors [6, 7]. Axions being potential dark-matter candidates [8–11], were originally hypothesized to exist as a solution to the strong CP problem [12–14] and later generalized to classes of axion-like particles (ALPs), see the review [15].

Cosmological and astrophysical constraints for ALPs are stringent, but it is also necessary to perform laboratory experiments in searches for axions or ALPs since these experiments are well-controlled, reproducible, and less model-dependent. There are several approaches of laboratory experiments based on axion-photon coupling, such as helioscopes, light-shining through walls interferometry, and solar-axion experiments as shown in the review [11]. Solar-axion experiments have been devised to detect the associated solar axions resonantly in terrestrial laboratories, like in the case of ^7Li [16], ^{57}Fe [17], and ^{83}Kr [18]. To cover higher mass regions with terrestrial sources, collider, and beam-dump facilities [19], nuclear reactor facilities [20] and radio-active-source based experiments are ongoing or proposed.

Among different proposed detection possibilities, the detection of axions through magnetic-dipole(M1)-decaying excited states (ESs) of nuclei has been proposed [21]. Here one looks for a missing γ in the ALP detector. These experiments have the advantage that they can be performed on the laboratory scale. The first such de-

tection experiment was proposed by the group of by the group of M. Minowa [6] using ^{139}Ce radioactive source surrounded by CsI:Tl crystal scintillator to tag X-rays and γ s. In this experiment, the M1 transition of interest is the $5/2_1^+ \rightarrow 7/2_1^+$ 165.86 keV transition shown in Fig. 1a. As shown in the figure, the initial $5/2_1^+$ state is fed by an allowed Gamow-Teller (GT) electron-capture (EC) transition from the $3/2_1^+$ ground state of ^{139}Ce , having a branching ratio (BR) that is practically 1. This EC decay can be detected by its X-ray or Auger-electron (AE) emission, thus tagging the unobservation of an M1 γ (or conversion electron (CE) from the internal conversion process) leading to a potential indirect detection of the emission of an ALP.

A severe experimental problem turns out to be the possible rare branching of the EC decay to the $7/2_1^+$ ground state (GS) of the daughter nucleus ^{139}La since this transition creates X-rays (or AEs) without emission of γ -rays, thus mimicking emission of an ALP. This experiment could set the upper limit $\Gamma_{\text{invisible}}/\Gamma_{\text{total}} < 9.70 \times 10^{-7}$ (95% C.L.) to the invisible transition rate relative to the total transition rate. Based on this measurement, an evaluated value of $5(5) \times 10^{-9}$ has been compiled in the NNDC database [22]. The GS transition is very much hindered by the fact that it is a 2^{nd} -forbidden non-unique (FNU) EC transition with the emission of an electron neutrino as a higher orbital angular momentum partial wave (see below for more details of these type of transitions). In these laboratory-scale experiments external backgrounds can be significantly lowered by going deep underground and using shielding materials, but the problem of this internal EC background still remains unresolved without dedicated experiments and/or reliable nuclear-structure calculations.

In addition to the case of ^{139}La , discussed above, there are other two known suitable candidates, namely ^{44}Sc and ^{57}Fe , for detection of new dark-matter particles such as ALPs (M1 and M2 transitions) [21], dark

* aagrah.a.agnihotri@student.jyu.fi

† jouni.t.suhonen@jyu.fi; Also at International Centre for Advanced Training and Research in Physics (CIFRA), P.O. Box MG12, 077125 Bucharest-Măgurele, Romania

‡ hongjooknu@gmail.com

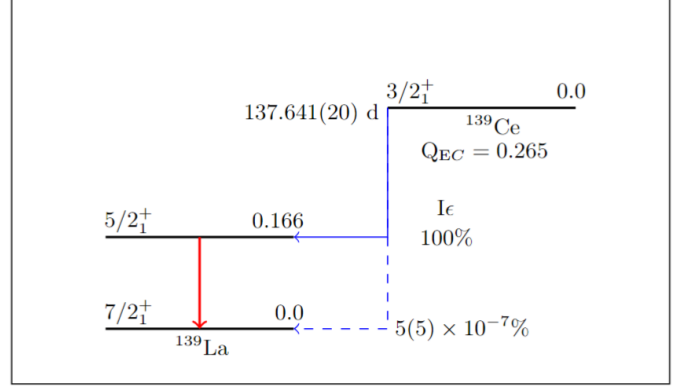
photons (E1 transition) [23], and anapoles (E2 transition) being constituents of anapole dark matter [24]. The electromagnetic (EM) decay and EC feeding schemes of these nuclei are depicted Fig. 1b and 1c, respectively. The known EC branches of these sources include the GT transitions $^{57}\text{Co}(7/2_1^-) \rightarrow ^{57}\text{Fe}^*(5/2_1^-)$ and $^{57}\text{Co}(7/2_1^-) \rightarrow ^{57}\text{Fe}^*(5/2_2^-)$, along with the 1st-FNU β transitions $^{44}\text{Ti}(0_1^+) \rightarrow ^{44}\text{Sc}^*(1_1^-)$ and $^{44}\text{Ti}(0_1^+) \rightarrow ^{44}\text{Sc}^*(0_1^-)$. In the former case we focus our attention to the EC branch with the strong feeding, namely the allowed transition $^{57}\text{Co}(7/2_1^-) \rightarrow ^{57}\text{Fe}^*(5/2_1^-)$, offering interesting M1 and E2 transitions for the studies of exotic dark-matter particles.

There are two major possibilities for dark-matter-particle searches through the EC transition $^{57}\text{Co}(7/2_1^-) \rightarrow ^{57}\text{Fe}^*(5/2_1^-)$, where rare unknown EC decays can serve as a background. The first approach involves searches for ALPs through the $^{57}\text{Fe}^*(5/2_1^-) \rightarrow ^{57}\text{Fe}^*(3/2_1^-)$ M1 transition with a 122.0614 keV γ emission, followed by the $^{57}\text{Fe}^*(3/2_1^-) \rightarrow ^{57}\text{Fe}(1/2_1^-)$ M1 transition with a 14.41300 keV γ emission. In the case of an APL signal, the 122.0614 keV γ emission would be missing, meaning that only X-rays (or AEs) and 14.41300 keV γ emissions would be observed. In this scenario the calculation of the rare ground-state-to-excited-state (GS-to-ES) EC branching $^{57}\text{Co}(7/2_1^-) \rightarrow ^{57}\text{Fe}^*(3/2_1^-)$ is crucial, as it will serve as background to the ALP signal. The second approach involves searches for anapoles through the $^{57}\text{Fe}^*(5/2_1^-) \rightarrow ^{57}\text{Fe}(1/2_1^-)$ E2 transition with a 136.4743 keV γ emission. In the case of an anapole signal, the 136.4743 keV γ would be missing, meaning that only X-ray (or AE) emissions would be observed. Here, the calculation of the ground-state-to-ground-state (GS-to-GS) EC branch is crucial as it will serve as background for the anapole signal. In addition to the above, the M1-decaying $3/2_1^-$ state is also a potential major source of ALP particles, where the ALP signal can be tagged using the γ -decays feeding this state.

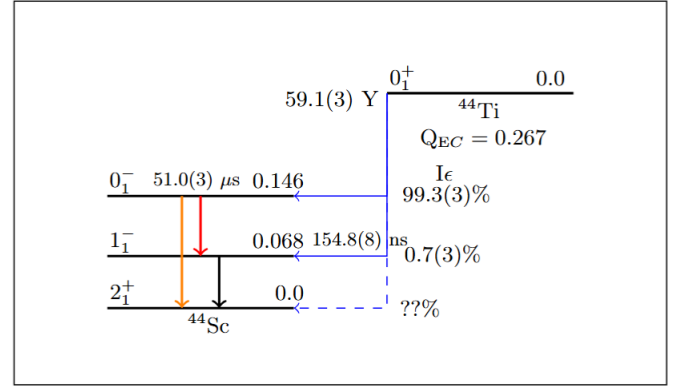
There are three major possibilities for dark-matter-particle searches through EC transitions from ^{44}Ti to states in ^{44}Sc . The first and second possibilities involve the EC transition $^{44}\text{Ti}(0_1^+) \rightarrow ^{44}\text{Sc}^*(0_1^-)$. The first approach is searching for ALPs through the $^{44}\text{Sc}^*(0_1^-) \rightarrow ^{44}\text{Sc}^*(1_1^-)$ M1 transition with a 78.337 keV γ emission, followed by the $^{44}\text{Sc}^*(1_1^-) \rightarrow ^{44}\text{Sc}(2_1^+)$ E1 transition with a 67.875 keV γ emission. In the case of an ALP signal, the 78.337 keV γ emission would be missing, meaning that only X-rays (or AEs) and 67.875 keV γ emissions would be observed. The second approach involves searches of an M2 ALP [21] through the $^{44}\text{Sc}^*(0_1^-) \rightarrow ^{44}\text{Sc}(2_1^+)$ M2 transition with a 146.212 keV γ emission. In the case of the presence of the M2 ALP, the 146.212 keV γ emission would be missing, indicating the presence of only X-rays (or AEs). In this case, calculation of the GS-to-GS EC branch is crucial as it will serve as background for the M2-ALP signal. The third possibility involves searching for a dark photon through the $^{44}\text{Sc}^*(1_1^-) \rightarrow ^{44}\text{Sc}(2_1^+)$ E1

FIG. 1: Decay schemes for the three sources considered in this Letter. M1 transitions are marked by bold red arrows for all decay schemes. E1 and M2 transitions in (b) are marked by bold dark green and orange arrows, respectively. The E2 transition in (c) is marked by bold brown arrow.

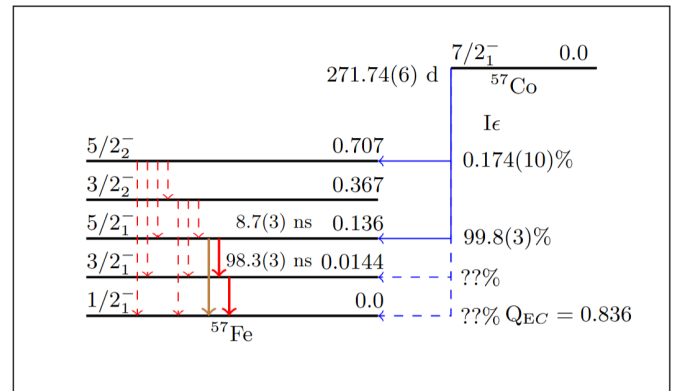
(a) EC decay scheme of ^{139}Ce .



(b) EC decay scheme of ^{44}Ti .



(c) EC decay scheme of ^{57}Co .



transition with a 67.875 keV γ emission. In the case of a dark photon signal, the 67.875 keV γ emission would be missing, meaning that only X-rays (or AEs) would be observed. As with the second possibility, calculation of the GS-to-GS EC branch is essential as it will serve as background for the dark-photon signal.

Experimentally, there are several critical points to consider for new dark-matter particle searches like those involving ALPs, dark photons and anapoles. First, the detector should have excellent energy resolution to accurately tag low-energy X-rays or AEs. Additionally, precise timing resolution is required to effectively distinguish signals from γ -rays and X-rays (or AEs) in the transitions of ^{44}Sc and ^{57}Fe , as some of these transitions involve nuclear isomeric states, as shown in Figures 1b and 1c respectively. This approach provides a powerful technique for dramatically reducing radioactive background. Moreover, the veto detector should achieve 100% efficiency to ensure that γ -rays are not mistakenly identified as new-particle signals. Finally, the detector setup should be located deep underground with low-background lead and copper shielding, similar to WIMP dark-matter searches, to minimize cosmic and environmental background interference.

Our focus in this article is the estimation of BRs for the unknown rare EC branches by using the nuclear shell model (NSM) and a reasonable range $g_A^{\text{eff}} = 0.5 - 1.27$ of effective values of the weak axial coupling. In addition to the unknown rare EC transitions, we also evaluate the known relevant GS-to-ES EC branches present in the decay of the source isotopes in order to validate our methodology for obtaining reasonable BR estimates.

The non-relativistic limit of the theory of β decays is well established and a detailed account is presented in [25]. A more concise and practical exposition of the treatment of forbidden β^+ /EC decays is given in [26]. The half-life value for pure EC decays, $t_{1/2}^{\text{EC}}$, is given as $t_{1/2}^{\text{EC}} = \kappa / \tilde{C}^{\text{EC}}$, where κ takes the value of 6289 s and \tilde{C}^{EC} is the integrated shape function which can be written as [26]

$$\tilde{C}^{\text{EC}} = \frac{\pi}{2} \sum_{x=1s,2s} n_x \beta_x^2 (p_{\nu_x} / m_e c)^2 C(p_{\nu_x}), \quad (1)$$

when considering the leading channels, namely K capture (1s) and L_1 capture (2s). Here n_x are relative occupancies for the respective orbitals, β_x are the electron Coulomb amplitudes, and p_{ν_x} is the momentum of the neutrino when the electron is captured from the atomic orbital x [26]. The shape factor $C(p_{\nu_x})$ used in Eq. (1), containing complicated combinations of phase-space factors and nuclear matrix elements (NMEs), is given for forbidden EC transitions in detail in [26].

Nuclear wave functions for the NMEs and EM observables were computed using the NSM computer program NuShellX@MSU [27]. The nuclei ^{44}Ti and ^{44}Sc were computed in the SDPFNP model space with the NOWPN interaction and ^{36}Ar core. The nucleus

^{57}Co was computed using the FPPN model space and GX1APN interaction. For ^{57}Fe , KB3GPN interaction was used in the FPPN model space with the truncation scheme of [28]. For ^{139}La and ^{139}Ce , the JJ55PN model space was used with the SN100PN interaction. Four protons are fixed in the $1g_{7/2}$ orbital for ^{139}Ce .

Comparison of the computed and experimental energies of levels in the nuclei ^{44}Ti , ^{44}Sc , ^{57}Co , ^{57}Fe , ^{139}Ce , and ^{139}La are given in Table I of the Supplemental Material [29]. In this material, in Table II, we also compare the computed values of magnetic dipole (μ) and electric quadrupole (Q) moments of the involved states with the available data. These moments are indicative of the quality of the wave functions of states involved in the EC and electromagnetic transitions [30, 31]. In the Supplemental Material we also compare the computed M1, E1, M2, and E2 transition probabilities, depicted in Fig. 1, and their mixing ratios, with the available data.

Predicting BRs and (partial) half-lives of β transitions using NSM-computed wave functions calls for the use of an effective value g_A^{eff} of the weak axial coupling [32]. g_A^{eff} is related to the quenching factor q as $q = g_A^{\text{eff}} / g_A$ [32], where $g_A = 1.276$ [33] is the free-nucleon value. The key inference we consider here is that for different branches of the EC decay of the parent nucleus, q is not unique. This follows from the fact that the g_A^{eff} is an artifact reflecting the incompleteness of the wave functions involved [34]. The more complete the state, the closer the value of q is to unity [34].

The validity of the above inference is justified when we look at the two Gamow-Teller (GT) branches of the decay of ^{57}Co : The GT transitions that populate the $5/2_1^-$ and $5/2_2^-$ levels in ^{57}Fe have BRs of 0.998(3) and 0.00174(10), respectively [22]. The branches are identical in a sense that the initial and final spin-parities J^π are the same. Also, the wave function of the initial state is common for both. The g_A^{eff} for these respective branches are found to be 1.25 and 0.548 for the GT matrix elements $M_{\text{GT}} = -0.1065$ and $M_{\text{GT}} = 0.0572$, respectively, when using the phase-space factors of [35]. This difference in quenching is due to the difference in the quality of final-state wave functions. In Table II of the Supplemental Material [29], it can be seen that for the $5/2_1^-$ state, the M1 moment μ is in very good agreement with the experimental value, justifying a near-unity q value of 0.982. Along the same lines, in the decay of ^{139}Ce , the GT transition populating the $5/2_1^+$ state with $\text{BR} \approx 1$ [22] turns out to have $g_A^{\text{eff}} = 0.914$ for $M_{\text{GT}} = 0.340$. This g_A^{eff} value is quite compatible with the relatively well-predicted EM moments of Table II of the Supplemental Material [29]. Based on all these examples, we conjecture that the quenched effective value g_A^{eff} appears as a free parameter for all β transitions. Therefore, for the aforementioned unknown rare EC branches, we make estimations of BRs and partial half-lives for a conservative interval $g_A^{\text{eff}} \in [0.5 - 1.27]$, found sufficient, e.g., in the works [32, 36, 37].

An additional free parameter, namely the small rel-

ativistic vector NME (sNME) appears for FNU decays [36–38]. In the cases where the sNMEs are fitted to experimental BRs, it is seen that there exist two values of sNMEs that reproduce a given BR [37, 39–41]. Since three out of four rare EC decays under study are FNU, for these cases values of sNME must be fixed as well. The problem of the sNME is solved by looking at the variation of the EC half-life with the value of sNME for a given g_A^{eff} . It turns out that for all g_A^{eff} , there is a unique sNME that maximizes the EC half-life and, in turn, minimizes the corresponding BR. This opens up a way for estimation of the lower limits for the BRs of the rare EC transitions which is valuable for future experiments.

In order to study closer the influence of the sNME on the BRs we can use as a testing ground the fact that the decay of the 0_1^+ GS of ^{44}Ti populates the excited states 1_1^- and 0_1^- in ^{44}Sc , with branching ratios 0.007(3) and 0.993(3), respectively. Both these branches are 1st FNU but the transition to the 0_1^- state does not depend on sNME [42] and thus can be left out of the discussion. However, the study of the 1_1^- branch can help locate the sNME that minimizes the BR relative to the two sNMEs that reproduce the experimental BR. The relevant sNME and g_A^{eff} values are given in table I.

TABLE I: Computed sNME values (sNME₁ and sNME₂) which reproduce the experimental BR of the $^{44}\text{Ti}(0_1^+) \rightarrow ^{44}\text{Sc}^*(1_1^-)$ transition and the sNME value sNME_{min} which minimizes the BR of this transition for the effective weak axial couplings of interest in this work. The CVC value of the sNME, sNME_{CVC}, is given for reference.

g_A^{eff}	sNME ₁	sNME ₂	sNME _{min}
0.5	-0.00535	-0.00094	-0.00314
0.6	-0.00596	-0.00154	-0.00375
0.7	-0.00656	-0.00215	-0.00435
0.8	-0.00717	-0.00275	-0.00496
0.9	-0.00777	-0.00336	-0.00556
1.0	-0.00838	-0.00396	-0.00617
1.1	-0.00898	-0.00457	-0.00678
1.2	-0.00959	-0.00517	-0.00738
1.27	-0.01001	-0.00560	-0.00780
sNME _{CVC} = -0.01350			

In table I it can be seen that sNME_{min} is always located in between NME₁ and NME₂. This means that sNME values larger or smaller than sNME_{min} produce larger branchings for all relevant g_A^{eff} . The CVC value of sNME, denoted as sNME_{CVC} in Table I, is also unique and can potentially give additional information on the physical value of sNME [36–38]. Yet, due to the lack of perfectly modeled wave functions, predictions using the CVC value usually fall short of reproducing experimental values of BRs, making the CVC value only a good reference in searches of the proper value of the sNME in different nuclear models [36–38]. This is also the case for the 1st FNU transition at hand, where sNME_{CVC} reproduces the

experimental BR for $g_A^{\text{eff}} > 1.276$.

For the rare EC transitions relevant for this work, BRs are tabulated in Table II. There we give the value sNME_{min}, minimizing the rare BR (BR_{min}) (and maximizing the half-life $t_{1/2,\text{max}}$), for the FNU GS-to-GS decays of ^{44}Ti and ^{139}Ce , and the FNU GS-to-ES and FU GS-to-GS decays of ^{57}Co . As can be seen, the BR_{min} changes smoothly with g_A^{eff} being smallest for $g_A^{\text{eff}} = 0.5$ for the GS-to-GS decays of ^{57}Co and ^{139}Ce , whereas for the GS-to-GS decay of ^{44}Ti the smallest value is achieved for $g_A^{\text{eff}} = 1.27$. For the GS-to-ES decay of ^{57}Co BR_{min} is achieved for a g_A value $g_A^{\text{eff}} = 0.65$ (in Table II the rounded-up numbers become the same for $g_A^{\text{eff}} = 0.6$ and $g_A^{\text{eff}} = 0.7$). Therefore, the most conservative estimates are the lowest BRs obtained, 4.72×10^{-9} (with the corresponding maximum half-life $t_{1/2,\text{max}} = 3.95 \times 10^{17}$ s) for the GS-to-GS decay of $^{44}\text{Ti}(0_1^+)$, 1.63×10^{-9} ($t_{1/2,\text{max}} = 1.44 \times 10^{16}$ s) for the GS-to-GS decay of $^{57}\text{Co}(7/2_1^-)$, 2.47×10^{-8} ($t_{1/2,\text{max}} = 9.51 \times 10^{14}$ s) for the GS-to-ES decay of $^{57}\text{Co}(7/2_1^-)$, and 1.00×10^{-9} ($t_{1/2,\text{max}} = 1.19 \times 10^{16}$ s) for the GS-to-GS decay of $^{136}\text{Ce}(3/2_1^+)$, and these are the ones suggested for the experiments. It should be noted here that for ^{139}Ce our result BR_{min} = 1.00×10^{-9} is well in line with the measured upper limit $\Gamma_{\text{invisible}}/\Gamma_{\text{total}} < 9.70 \times 10^{-7}$ (95% C.L.) [6], and compiled value of $5(5) \times 10^{-9}$ [22].

In summary, we give for the first time theoretical estimates for the minimum branching ratios of the rare ground-state-to-ground-state second-forbidden electron-capture transitions $^{44}\text{Ti}(0_1^+) \rightarrow ^{44}\text{Sc}(2_1^+)$, $^{57}\text{Co}(7/2_1^-) \rightarrow ^{57}\text{Fe}(1/2_1^-)$, and $^{139}\text{Ce}(3/2_1^+) \rightarrow ^{139}\text{La}(7/2_1^+)$, and for the rare ground-state-to-excited-state second-forbidden electron-capture transition $^{57}\text{Co}(7/2_1^-) \rightarrow ^{57}\text{Fe}^*(3/2_1^-)$. The nuclear-structure calculations have been done exploiting well-established nuclear shell-model Hamiltonians and an advanced theory of β decay. The obtained minimum branching ratios are 4.72×10^{-9} for the decay of Ti, 1.63×10^{-9} (GS-to-GS) and 2.47×10^{-8} (GS-to-ES) for the decays of Co, and 1.00×10^{-9} for the decay of Ce, the last fully compatible with the available experimental upper limit of the branching ratio. It is conjectured that in the absence of experimental measurements of these decay branches, these estimates are of utmost importance for terrestrial searches of exotic new particles, like axionic dark matter, dark photons, and anapole dark matter exploiting nuclear transitions, as they can potentially mimic detection rates of these particles in the related experiments.

ACKNOWLEDGMENTS

J.S. acknowledges support from project PNRR-I8/C9-CF264, Contract No. 760100/23.0 5.2023 of the Romanian Ministry of Research, Innovation and Digitization (the NEPTUN project). H.J. Kim acknowledges support by the National Research Foundation of Korea (NRF)

TABLE II: Values of sNMEs ($s\text{NME}_{\min}$) which minimize the rare BR (BR_{\min}) (and hence maximize the corresponding half-life $t_{1/2,\max}$) for the effective weak axial couplings of interest in this work. The transition $^{57}\text{Co}(7/2_1^-) \rightarrow ^{57}\text{Fe}(1/2_1^-)$ is FU and thus independent of sNME. The lowest values of BR are highlighted, and they can serve as conservative estimates for experiments.

	$^{44}\text{Ti}(0_1^+) \rightarrow ^{44}\text{Sc}(2_1^+)$ 2 nd -FNU		$^{57}\text{Co}(7/2_1^-) \rightarrow ^{57}\text{Fe}^*(3/2_1^-)$ 2 nd -FNU		$^{57}\text{Co}(7/2_1^-) \rightarrow ^{57}\text{Fe}(1/2_1^-)$ 2 nd -FU		$^{139}\text{Ce}(3/2_1^+) \rightarrow ^{139}\text{La}(7/2_1^+)$ 2 nd -FNU	
g_A^{eff}	sNME _{min}	BR _{min}	sNME _{min}	BR _{min}	BR	sNME _{min}	BR _{min}	
0.5	-0.0203	6.15E-9	0.0293	2.52E-8	1.63E-9	-0.136	1.00E-9	
0.6	-0.0238	5.95E-9	0.0343	2.47E-8	2.35E-9	-0.163	1.12E-9	
0.7	-0.0272	5.76E-9	0.0393	2.47E-8	3.19E-9	-0.191	1.25E-9	
0.8	-0.0306	5.57E-9	0.0442	2.52E-8	4.17E-9	-0.219	1.38E-9	
0.9	-0.0341	5.38E-9	0.0492	2.61E-8	5.28E-9	-0.246	1.53E-9	
1.0	-0.0375	5.20E-9	0.0542	2.74E-8	6.52E-9	-0.274	1.68E-9	
1.1	-0.0409	5.02E-9	0.0592	2.91E-8	7.89E-9	-0.302	1.84E-9	
1.2	-0.0444	4.84E-9	0.0642	3.13E-8	9.39E-9	-0.330	2.01E-9	
1.27	-0.0468	4.72E-9	0.0676	3.31E-8	1.05E-8	-0.349	2.13E-9	

TABLE III: Glossary

Acronym/symbol	Defination
AE	Auger electron
ALP	Axion-like particle
BR	Branching ratio
BSMP	Beyond the standard model physics
CE	Conversion electron
CVC	Conserved vector current
EC	Electron capture
EM	Electromagnetic
ES	Excited state
FNU	Forbidden non-unique
FU	Forbidden unique
GS	Ground state
GT	Gamow-Teller
NSM	Nuclear shell model
M1	Magnetic Dipole
μ	Magnetic dipole moment
NME	Nuclear matrix element
Q	Electric quadrupole moment
sNME	small relativistic vector NME
sNME _{min}	sNME that minimizes the BR
sNME _{CVC}	CVC value of sNME

grant, funded by the Korean government (MSIT), Contract No. RS-2024-00348317. We acknowledge grants of computer capacity from the Finnish Grid and Cloud Infrastructure (persistent identifier urn:nbn:fi:research-infras-2016072533) and the support by CSC – IT Center for Science, Finland, for the generous computational resources.

- [1] H. Ejiri, J. Suhonen, and K. Zuber, Neutrino–nuclear responses for astro-neutrinos, single beta decays and double beta decays, *Physics Reports* **797**, 1 (2019).
- [2] M. Brodeur *et al.*, Nuclear β decay as a probe for physics beyond the Standard Model (2023), arXiv:2301.03975 [nucl-ex].
- [3] M. González-Alonso, O. Naviliat-Cuncic, and N. Severijns, New physics searches in nuclear and neutron β decay, *Progress in Particle and Nuclear Physics* **104**, 165 (2019).
- [4] V. Guadilla, A. Algora, M. Estienne, M. Fallot, W. Gelletly, A. Porta, L.-M. Rigalleau, and J.-S. Stutzmann, First measurements with a new β -electron detector for spectral shape studies, *Journal of Instrumentation* **19**, P02027.
- [5] L. Pagnanini *et al.*, Array of cryogenic calorimeters to evaluate the spectral shape of forbidden β -decays: the ACCESS project, *Eur. Phys. J. Plus* **138**, 445 (2023).
- [6] M. Minowa, Y. Inoue, T. Asanuma, and M. Imamura, Invisible axion search in ^{139}La M1 transition, *Phys. Rev. Lett.* **71**, 4120 (1993).
- [7] R. Massarczyk, P.-H. Chu, and S. R. Elliott, Axion emission from nuclear magnetic dipole transitions, *Phys. Rev. D* **105**, 015031 (2022).
- [8] J. Preskill, M. B. Wise, and F. Wilczek, *Cosmology of*

- the invisible axion, *Physics Letters B* **120**, 127 (1983).
- [9] L. Abbott and P. Sikivie, A cosmological bound on the invisible axion, *Physics Letters B* **120**, 133 (1983).
- [10] M. Dine and W. Fischler, The not-so-harmless axion, *Physics Letters B* **120**, 137 (1983).
- [11] I. G. Irastorza and J. Redondo, New experimental approaches in the search for axion-like particles, *Progress in Particle and Nuclear Physics* **102**, 89 (2018).
- [12] R. D. Peccei and H. R. Quinn, CP Conservation in the Presence of Pseudoparticles, *Phys. Rev. Lett.* **38**, 1440 (1977).
- [13] S. Weinberg, A New Light Boson?, *Phys. Rev. Lett.* **40**, 223 (1978).
- [14] F. Wilczek, Problem of Strong P and T Invariance in the Presence of Instantons, *Phys. Rev. Lett.* **40**, 279 (1978).
- [15] K. Choi, S. H. Im, and C. Sub Shin, Recent Progress in the Physics of Axions and Axion-Like Particles, *Ann. Rev. Nucl. Part. Sci.* **71**, 225 (2021), arXiv:2012.05029 [hep-ph].
- [16] P. Belli, R. Bernabei, F. Cappella, R. Cerulli, F. A. Danevich, A. Incicchitti, V. V. Kobychev, *et al.*, Search for ${}^7\text{Li}$ solar axions using resonant absorption in LiF crystal: Final results, *Phys. Lett. B* **711**, 41 (2012).
- [17] A. V. Derbin, V. N. Muratova, D. A. Semenov, and E. V. Unzhakov, New limit on the mass of 14.4 keV solar axion emitted in an M1 transition in ${}^{57}\text{Fe}$ nuclei, *Phys. At. Nucl.* **74**, 596 (2011).
- [18] K. Jakovčić, Z. Krecak, M. Krčmar, and A. Ljubčić, A search for solar hadronic axions using ${}^{83}\text{Kr}$, *Rad. Phys. Chem.* **71**, 793 (2004).
- [19] M. Bauer, M. Heiles, M. Neubert, and A. Thamm, Axion-like particles at future colliders., *Eur. Phys. J. C* **79**, 74 (2019).
- [20] J. B. Dent, B. Dutta, D. Kim, S. Liao, R. Mahapatra, K. Sinha, and A. Thompson, New Directions for Axion Searches via Scattering at Reactor Neutrino Experiments, *Phys. Rev. Lett.* **124**, 211804 (2020).
- [21] T. W. Donnelly, S. J. Freedman, R. S. Lytel, R. D. Peccei, and M. Schwartz, Do axions exist?, *Phys. Rev. D* **18**, 1607 (1978).
- [22] ENSDF database, National Nuclear Data Center (NNDC) (2024).
- [23] A. Filippi and M. De Napoli, Searching in the dark: the hunt for the dark photon, *Reviews in Physics* **5**, 100042 (2020).
- [24] S. Y. Choi, J. Jeong, D. W. Kang, and S. Shin, Hunting for hypercharge anapole dark matter in all spin scenarios, *Phys. Rev. D* **109**, 096001 (2024).
- [25] H. O. Behrens and W. Bühring, *Electron radial wave functions and nuclear beta-decay* (Oxford University Press, 1982).
- [26] E. Ydrefors, M. Mustonen, and J. Suhonen, MQPM description of the structure and beta decays of the odd $A=95,97$ Mo and Tc isotopes, *Nuclear Physics A* **842**, 33 (2010).
- [27] B. Brown and W. Rae, The Shell-Model Code NuShellX@MSU, *Nuclear Data Sheets* **120**, 115 (2014).
- [28] F.T. Avignone III, R. Creswick, J. Vergados, P. Pirinen, P. Srivastava, and J. Suhonen, Estimating the flux of the 14.4 keV solar axions, *Journal of Cosmology and Astroparticle Physics* **2018** (01), 021.
- [29] See Supplemental Material at [URL], for information on electromagnetic observables important for justifications of arguments in the main text, This material includes Refs.[22, 43].
- [30] T. Suzuki, R. Fujimoto, and T. Otsuka, Gamow-Teller transitions and magnetic properties of nuclei and shell evolution, *Phys. Rev. C* **67**, 044302 (2003).
- [31] Y. Fujita, H. Fujita, and Y. Tanumura, Analogous Gamow-Teller and M1 Transitions in $T_z = \pm\frac{1}{2}$ Mirror Nuclei and in $T_z = \pm 1, 0$ Triplet Nuclei relevant to Low-energy Super GT state, *EPJ Web Conf.* **178**, 05001 (2018).
- [32] J. T. Suhonen, Value of the Axial-Vector Coupling Strength in β and $\beta\beta$ Decays: A Review, *Frontiers in Physics* **5** (2017).
- [33] B. Märkisch, H. Mest, H. Saul, X. Wang, H. Abele, D. Dubbers, M. Klopff, A. Petoukhov, C. Roick, T. Soldner, and D. Werder, Measurement of the Weak Axial-Vector Coupling Constant in the Decay of Free Neutrons Using a Pulsed Cold Neutron Beam, *Phys. Rev. Lett.* **122**, 242501 (2019).
- [34] P. Gysbers, G. Hagen, J. D. Holt, G. R. Jansen, T. D. Morris, P. Navratil, T. Papenbrock, S. Quaglioni, A. Schwenk, S. R. Stroberg, and K. A. Wendt, Discrepancy between experimental and theoretical β -decay rates resolved from first principles, *Nat. Phys.* **15**, 428 (2019).
- [35] N. Gove and M. Martin, Log-f tables for beta decay, *Atomic Data and Nuclear Data Tables* **10**, 205 (1971).
- [36] J. Kostensalo, J. Suhonen, J. Volkmer, S. Zatschler, and K. Zuber, Confirmation of g_A quenching using the revised spectrum-shape method for the analysis of the ${}^{113}\text{Cd}$ β -decay as measured with the COBRA demonstrator, *Physics Letters B* **822**, 136652 (2021).
- [37] L. Pagnanini *et al.*, Simultaneous Measurement of Half-Life and Spectral Shape of ${}^{115}\text{In}$ β -decay with an Indium Iodide Cryogenic Calorimeter (2024), arXiv:2401.16059 [nucl-ex].
- [38] A. Kumar, P. C. Srivastava, J. Kostensalo, and J. Suhonen, Second-forbidden nonunique β^- decays of ${}^{24}\text{Na}$ and ${}^{36}\text{Cl}$ assessed by the nuclear shell model, *Phys. Rev. C* **101**, 064304 (2020).
- [39] J. Kostensalo, E. Lisi, A. Marrone, and J. Suhonen, ${}^{113}\text{Cd}$ β -decay spectrum and g_A quenching using spectral moments, *Phys. Rev. C* **107**, 055502 (2023).
- [40] M. Ramalho and J. Suhonen, Computed total β -electron spectra for decays of Pb and Bi in the ${}^{220,222}\text{Rn}$ radioactive chains, *Phys. Rev. C* **109**, 014326 (2024).
- [41] M. Ramalho and J. Suhonen, g_A -sensitive β spectral shapes in the mass $A = 86 - 99$ region assessed by the nuclear shell model, *Phys. Rev. C* **109**, 034321 (2024).
- [42] D. E. Alburger and E. K. Warburton, First-forbidden $0^+ \rightarrow 0^-, 1^-$ electron capture of ${}^{44}\text{Ti}$, *Phys. Rev. C* **38**, 1843 (1988).
- [43] J. Suhonen, *From Nucleons to Nucleus* (Springer Berlin, Heidelberg, 2007).